

# Contribution of off-resonant states to the phase noise of quantum dot lasers

CHENG WANG,<sup>1,2,3,\*</sup> JUN-PING ZHUANG,<sup>2</sup> FRÉDÉRIC GRILLOT,<sup>3,4</sup>  
AND SZE-CHUN CHAN<sup>2,5</sup>

<sup>1</sup>School of Information Science and Technology, ShanghaiTech University, Shanghai 201210, China

<sup>2</sup>Department of Electronic Engineering, City University of Hong Kong, Hong Kong, China

<sup>3</sup>CNRS LTCI, Télécom ParisTech, Université Paris Saclay, 46 rue Barrault, F-75634 Paris Cedex 13, France

<sup>4</sup>Center for High Technology Materials, University of New Mexico, 1313 Goddard St. SE, Albuquerque, NM 87106-4343, USA

<sup>5</sup>State Key Laboratory of Millimeter Waves, City University of Hong Kong, Hong Kong, China

\*wangcheng1@shanghaitech.edu.cn

**Abstract:** The phase noise of quantum dot lasers is investigated theoretically by coupling the Langevin noise sources into the rate equations. The off-resonant populations in the excited state and in the carrier reservoir contribute to the phase noise of ground-state emission lasers through the phase-amplitude coupling effect. This effect arises from the optical-noise induced carrier fluctuations in the off-resonant states. In addition, the phase noise has low sensitivity to the carrier scattering rates.

© 2016 Optical Society of America

**OCIS codes:** (250.5960) Semiconductor lasers; (250.5590) Quantum-well, -wire and -dot devices; (270.2500) Fluctuations, relaxations, and noise.

## References and links

1. M. Nakazawa, K. Kikuchi, and T. Miyazaki, *High Spectral Density Optical Communication Technologies* (Springer, 2010).
2. J. Kahn, "Modulation and detection techniques for optical communication systems," in *Optical Amplifiers and Their Applications/Coherent Optical Technologies and Applications*, Technical Digest (Optical Society of America, 2006), paper CThC1.
3. K. Kikuchi, "Fundamentals of coherent optical fiber communications," *J. Lightwave Technol.* **34**(1), 157–179 (2016).
4. M. Okai, M. Suzuki, and T. Taniwatori, "Strained multi-quantum-well corrugation-pitch-modulated distributed feedback laser with ultranarrow (3.6 kHz) spectral linewidth," *Electron. Lett.* **29**(19), 1696–1697 (1993).
5. V. Weldon, P. Pineda-Vadillo, M. Lynch, R. Phelan, and J. F. Donegan, "A novel discrete mode narrow linewidth laser diode for spectroscopic based gas sensing in the 1.5  $\mu\text{m}$  region," *Appl. Phys. B* **109**(3), 433–440 (2012).
6. C. T. Santis, S. T. Steger, Y. Vilenchik, A. Vasilyev, and A. Yariv, "High-coherence semiconductor lasers based on integral high-Q resonators in hybrid Si/III-V platforms," *Proc. Natl. Acad. Sci.* **111**(8), 2879–2884 (2014).
7. B. Kelly, R. Phelan, D. Jones, C. Herbert, J. O'Carroll, M. Rensing, J. Wendelboe, C.B. Watts, A. Kaszubowska-Anandarajah, P. Perry, C. Guignard, L.P. Barry, and J. O'Gorman, "Discrete mode laser diodes with very narrow linewidth emission," *Electron. Lett.* **43**(23), 1 (2007).
8. D. G. Deppe, K. Shavritranuruk, G. Ozgur, H. Chen, and S. Freisem, "Quantum dot laser diode with low threshold and low internal loss," *Electron. Lett.* **45**(1), 54–56 (2009).
9. G. T. Liu, A. Stintz, H. Li, K. J. Malloy, L. F. Lester, "Extremely low room-temperature threshold current density diode lasers using InAs dots in In<sub>0.15</sub>Ga<sub>0.85</sub>As quantum well," *Electron. Lett.* **35**(14), 1163–1165 (1999).
10. L. V. Asryan and S. Luryi, "Temperature-insensitive semiconductor quantum dot laser," *Solid State Electron.* **47**(2), 205–212 (2003).
11. S. S. Mikhlin, A. R. Kovsh1, I. L. Krestnikov1, A. V. Kozhukhov1, D. A. Livshits1, N. N. Ledentsov1, Y. M. Shernyakov, I. I. Novikov, M. V. Maximov, V. M. Ustinov, and Z. I. Alferov, "High power temperature-insensitive 1.3  $\mu\text{m}$  InAs/InGaAs/GaAs quantum dot lasers," *Semicond. Sci. Technol.* **20**(5), 340 (2005).
12. D. O'Brien, S. P. Hegarty, G. Huyet, and A. V. Uskov, "Sensitivity of quantum-dot semiconductor lasers to optical feedback," *Opt. Lett.* **29**(10), 1072–1074 (2004).
13. H. G. Schuster and K. Lüdge, *Nonlinear Laser Dynamics: From Quantum Dots to Cryptography* (Wiley, 2012).
14. S. M. Chen, W. Li, J. Wu, Q. Jiang, M. Tang, S. Shutts, S. N. Elliott, A. Sobiesierski, A. J. Seeds, I. Ross, P. M. Smowton, and H. Liu, "Electrically pumped continuous-wave III–V quantum dot lasers on silicon," *Nature Photon.* **10**(5), 307–311 (2016).

15. H. Su and L. F. Lester, "Dynamic properties of quantum dot distributed feedback lasers: high speed, linewidth and chirp," *J. Phys. D: Appl. Phys.* **38**(13), 2112 (2005).
16. Z. G. Lu, P. J. Poole, J. R. Liu, P. J. Barrios, Z. J. Jiao, G. Pakulski, D. Poitras, D. Goodchild, B. Rioux, and A. J. SpringThorpe, "High-performance 1.52  $\mu\text{m}$  InAs/InP quantum dot distributed feedback laser," *Electron. Lett.* **47**(14), 818–819 (2011).
17. A. Becker, V. Sichkovskiy, M. Bjelica, O. Eyal, P. Baum, A. Rippen, F. Schnabel, B. Witzigmann, G. Eisenstein, and J. P. Reithmaier, "Narrow-linewidth 1.5- $\mu\text{m}$  quantum dot distributed feedback lasers," *Proc. SPIE* **9767**, 97670Q (2016).
18. C. H. Henry, "Theory of the linewidth of semiconductor lasers," *IEEE J. Quantum Electron.* **18**(2), 259–264 (1982).
19. M. Osinski and J. Buus, "Linewidth broadening factor in semiconductor lasers—An overview," *IEEE J. Quantum Electron.* **23**(1), 9–29 (1987).
20. L. A. Coldren, S. W. Corzine, and M. L. Mashanovitch, *Diode Lasers and Photonic Integrated Circuits* (Wiley, 2012).
21. B. W. Hakki and T. L. Paoli, "Gain spectra in GaAs double-heterostructure injection lasers," *J. Appl. Phys.* **46**(3), 1299–1306 (1975).
22. C. Harder, K. Vahala, and A. Yariv, "Measurement of the linewidth enhancement factor  $\alpha$  of semiconductor lasers," *Appl. Phys. Lett.* **42**(4), 328–330 (1983).
23. J. G. Provost and F. Grillot, "Measuring the chirp and the linewidth enhancement factor of optoelectronic devices with a Mach–Zehnder interferometer," *IEEE Photon. J.* **3**(3), 476–488 (2011).
24. A. Villafranca, J. A. Lazato, I. Salinas, and I. Garces, "Measurement of the linewidth enhancement factor in DFB Lasers using a high-resolution optical spectrum analyzer," *IEEE Photon. Technol. Lett.* **17**(11), 2268–2270 (2005).
25. C. Wang, K. Schires, M. Osinski, P. J. Poole, and F. Grillot, "Thermally insensitive determination of the linewidth broadening factor in nanostructured semiconductor lasers using optical injection locking," *Sci. Rep.* **6**, 27825 (2016).
26. G. Giuliani, S. Donati, A. Villafranca, J. Lasobras, I. Garces, M. Chacinski, R. Schatz, C. Kouloumentas, D. Klonidis, I. Tomkos, P. Landais, R. Escorihuela, J. Rorison, J. Pozo, A. A. Fiore, P. Moreno, M. Rossetti, W. Elsässer, J. V. Staden, G. Huyet, M. Saarinen, M. Pessa, P. Leinonen, V. Vilokinen, M. Sciamanna, J. Danckaert, K. Panajotov, T. Fordell, A. Lindberg, J. F. Hayau, J. Poette, P. Besnard, F. Grillot, M. Pereira, R. Nelander, A. Wacker, A. Tredicucci, and R. Green, "Round-robin measurements of linewidth enhancement factor of semiconductor lasers in COST 288 Action," in *CLEO/Europe and IQEC 2007 Conference Digest*, (Optical Society of America, 2007), paper CB9-2.
27. Z. Mi and P. Bhattacharya, "DC and dynamic characteristics of p-doped and tunnel injection 1.65-InAs quantum-dash lasers grown on InP (001)," *IEEE J. Quantum Electron.* **42**(12), 1224–1232 (2006).
28. S. S. Bhowmick, M. Z. Baten, T. Frost, B. S. Ooi, and P. Bhattacharya, "High performance InAs/InP quantum dot 1.55  $\mu\text{m}$  tunnel injection laser," *IEEE J. Quantum Electron.* **50**(1), 7–14 (2014).
29. B. Dagens, A. Markus, J. X. Chen, J. G. Provost, D. Make, O. Le Gouezigou, J. Landreau, A. Fiore, and B. Thedrez, "Giant linewidth enhancement factor and purely frequency modulated emission from quantum dot laser," *Electron. Lett.* **41**(6), 323–324 (2005).
30. A. Martinez, K. Merghem, S. Bouchoule, G. Moreau, A. Ramdane, J. G. Provost, F. Alexandre, F. Grillot, O. Dehaese, R. Piron, and S. Lualiche, "Dynamic properties of InAs/InP (311B) quantum dot Fabry-Perot lasers emitting at 1.52- $\mu\text{m}$ ," *Appl. Phys. Lett.* **93**(2), 021101 (2008).
31. S. Melnik, G. Huyet, and A. V. Uskov, "The linewidth enhancement factor  $\alpha$  of quantum dot semiconductor lasers," *Opt. Express* **14**(7), 2950–2955 (2006).
32. C. Wang, F. Grillot, and J. Even, "Impacts of wetting layer and excited state on the modulation response of quantum-dot lasers," *IEEE J. Quantum Electron.* **48**(9), 1144–1150 (2012).
33. B. Ohnesorge, M. Albrecht, J. Oshinowo, A. Forchel, and Y. Arakawa, "Rapid carrier relaxation in self-assembled  $\text{In}_x\text{Ga}_{1-x}\text{As}/\text{GaAs}$  quantum dots," *Phys. Rev. B* **54**(16), 11532 (1996).
34. I. V. Ignatiev, I. E. Kozin, S. V. Nair, H. W. Ren, S. Sugou, and Y. Masumoto, "Carrier relaxation dynamics in InP quantum dots studied by artificial control of nonradiative losses," *Phys. Rev. B* **61**(23), 15633 (2000).
35. K. Veselinov, F. Grillot, C. Cornet, J. Even, A. Bekiarski, M. Gioannini, and S. Lualiche, "Analysis of double laser emission occurring in 1.55  $\mu\text{m}$  InAs-InP (113) B quantum dot laser," *IEEE J. Quantum Electron.* **43**(9), 810–816 (2007).
36. L. V. Asryan, Y. C. Wu, and R. A. Suris, "Analysis of double laser emission occurring in 1.55  $\mu\text{m}$  InAs-InP (113) B quantum dot laser," *Appl. Phys. Lett.* **98**(13), 131108 (2011).
37. C. Wang, M. Osinski, J. Even, and F. Grillot, "Phase-amplitude coupling characteristics in directly modulated quantum dot lasers," *Appl. Phys. Lett.* **105**(22), 221114 (2014).
38. C. Wang, B. Lingnau, K. Lüdge, J. Even, and F. Grillot, "Enhanced dynamic performance of quantum dot semiconductor lasers operating on the excited state," *IEEE J. Quantum Electron.* **50**(9), 1–9 (2014).
39. A. Markus, J. Chen, O. Gauthier-Lafaye, J. G. Provost, C. Paranthoën, and A. Fiore, "Impact of intraband relaxation on the performance of a quantum-dot laser," *IEEE J. Sel. Top. Quantum Electron.* **9**(5), 1308–1314 (2003).
40. B. Lingnau, W. W. Chow, E. Schöll, and K. Lüdge, "Feedback and injection locking instabilities in quantum-dot lasers: a microscopically based bifurcation analysis," *New J. Phys.* **15**(9), 093031 (2003).
41. M. Ahmed, M. Yamada, and M. Saito, "Numerical modeling of intensity and phase noise in semiconductor lasers," *IEEE J. Quantum Electron.* **37**(12), 1600–1610 (2001).
42. C. H. Henry, "Phase noise in semiconductor lasers," *J. Lightwave Technol.* **4**(3), 298–311 (1986).

43. T. B. Simpson and J. M. Liu, "Spontaneous emission, nonlinear optical coupling, and noise in laser diodes," *Opt. Commun.* **112**(1-2), 43–47 (1994).
44. J. Ohtsubo, *Semiconductor Lasers: Stability, Instability and Chaos* (Springer, 2012).
45. K. Kikuchi, "Effect of 1/f-type FM noise on semiconductor-laser linewidth residual in high-power limit," *IEEE J. Quantum Electron.* **25**(4), 684–688 (1989).
46. G. D. Domenico, S. Schilt, and P. Thomann, "Simple approach to the relation between laser frequency noise and laser line shape," *Appl. Opt.* **49**(25), 4801–4807 (2010).
47. F. Girardin, G. H. Duan, and P. Gallion, "Linewidth rebroadening due to nonlinear gain and index induced by carrier heating in strained quantum-well lasers," *IEEE Photon. Technol. Lett.* **8**(3), 334–336 (1996).
48. M. Gioannini and I. Montrosset, "Numerical analysis of the frequency chirp in quantum-dot semiconductor lasers," *IEEE J. Quantum Electron.* **43**(10), 941–949 (2007).
49. M. Gong, K. Duan, C. F. Li, R. Magri, G. A. Narvaez, and L. He, "Electronic structure of self-assembled InAs/InP quantum dots: comparison with self-assembled InAs/GaAs quantum dots," *Phys. Rev. B* **77**(4), 045326 (2008).
50. B. Lingnau, K. Lüdge, W. W. Chow, and E. Schöll, "Influencing modulation properties of quantum-dot semiconductor lasers by carrier lifetime engineering," *Appl. Phys. Lett.* **101**(13), 131107 (2012).
51. J. Pausch, C. Otto, E. Tylaite, N. Majer, E. Schöll, and Kathy Lüdge, "Optically injected quantum dot lasers: impact of nonlinear carrier lifetimes on frequency-locking dynamics," *New J. Phys.* **14**(5), 053018 (2012).
52. B. Lingnau, W. W. Chow, and K. Lüdge, "Amplitude-phase coupling and chirp in quantum-dot lasers: influence of charge carrier scattering dynamics," *Opt. Express* **22**(5), 4867–4879 (2014).
53. J. M. Garcia, G. Medeiros-Ribeiro, K. Schmidt, T. Ngo, J. L. Feng, A. Lorke, J. Kotthaus, and P. M. Petroff, "Intermixing and shape changes during the formation of InAs self-assembled quantum dots," *Appl. Phys. Lett.* **71**(14), 2014–2016 (1997).
54. T. Raz, D. Ritter, and G. Bahir, "Formation of InAs self-assembled quantum rings on InP," *Appl. Phys. Lett.* **82**(11), 1706–1708 (2003).
55. J. Even and S. Loualiche, "Exact analytical solutions describing quantum dot, ring and wire wavefunctions," *J. Phys. A, Math. General* **37**(27), L289–L294 (2004).

## 1. Introduction

With the increasing demand of transmission capacity in optical communication systems, coherent communication technology has been attracting intensive studies [1]. The coherent system can restore both the amplitude and the phase information of optical signals, while it is sensitive to the phase (frequency) noise of both transmitters and local oscillators, which strongly affects the bit error rates at the receiver [2, 3]. Therefore, developing low-noise semiconductor laser sources has become a crucial endeavor. The phase noise of semiconductor lasers is often quantified by the optical linewidth. Commercial quantum well (Qwell) lasers usually exhibit optical linewidths of a few MHz. In order to reduce the optical linewidth to the kHz range, continuous efforts have been made by increasing the quality factor of the laser cavity, tailoring a specific grating structure, and reducing the spontaneous emission into the lasing mode [4–7]. One alternative approach is to improve the active medium of semiconductor lasers through incorporating quantum dot (Qdot) structures. Qdot semiconductor lasers hold the promise to substitute their Qwell counterparts, owing to their superior characteristics such as low threshold current density [8, 9], good temperature stability [10, 11], high tolerance against optical feedback [12, 13], as well as the ability of direct growth on silicon substrates [14]. In terms of optical linewidth, Su and Lester reported an InAs/GaAs Qdot laser with a narrow linewidth around 500 kHz [15]. Lu *et al.* demonstrated an InAs/InP Qdot laser with a linewidth less than 150 kHz [16]. Recently, a minimum linewidth of 110 kHz was achieved in an InP-based Qdot laser [17]. The linewidths of these Qdot lasers are about one order of magnitude smaller than those of Qwell lasers, which is desirable for applications in coherent communication systems.

On one hand, the phase noise in semiconductor lasers arises from the spontaneous emission, which introduces the *Schawlow-Townes* linewidth  $\Delta\nu_{ST}$ . On the other hand, the optical linewidth  $\Delta\nu_{OL}$  is broadened by phase-amplitude coupling effect, which is characterized by the linewidth broadening factor (LBF)  $\alpha$  [18, 19]:

$$\Delta\nu_{OL} = \Delta\nu_{ST} (1 + \alpha^2) \quad (1)$$

Qwell lasers usually exhibit typical LBF values of 2.0–5.0 for both below- and above-threshold conditions [20]. In contrast, Qdot lasers exhibit a wide range of LBF values relying on the bias conditions and the various measurement techniques [21–26]. Qdot lasers biased below the lasing threshold measured by the *Hakki-Paoli* method do exhibit near-zero LBFs [27, 28]. However, the above-threshold LBF of Qdot lasers measured by *FM/AM* method can be relatively high up to over 10 [29, 30]. On the other hand, there is no report on the LBF of Qdot lasers measured from the spectral linewidth yet, to the best of our knowledge [24]. In theory, Melnik and Huyet studied the LBF and the linewidth of Qdot lasers considering the free carrier plasma effects in the carrier reservoir (RS) [31]. However, the contribution of populations in the excited state (ES) was not considered. In this work, we investigate the phase noise of Qdot lasers taking into account off-resonant populations both in the RS and in the ES. It is found that the ES dominates the contribution to the phase noise due to the stronger optical-noise induced carrier fluctuation than that in the RS. In addition, the phase noise of Qdot lasers has low sensitivity to the carrier capture and relaxation rates.

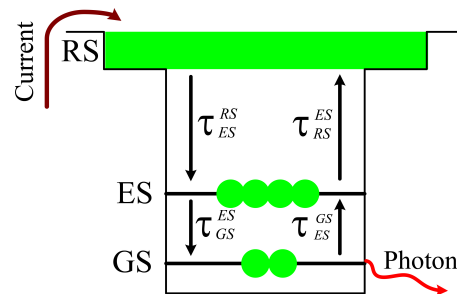


Fig. 1. Exciton electronic structure of the Qdot laser.

## 2. Rate equation model of Qdot lasers

Figure 1 illustrates the electronic structure of the Qdot laser, where charged electrons and holes are treated as neutral excitons [32]. The carriers are assumed to be directly injected into the two-dimensional carrier reservoir (RS) from the electrodes. Some carriers in the RS are captured into the excited state (ES) of dots with a capture time  $\tau_{ES}^{RS}$ , which is determined by Auger- and phonon-assisted scattering processes [33, 34]. The carriers then relax from the ES to the ground state (GS) with a relaxation time  $\tau_{GS}^{ES}$ . On the other hand, some carriers will escape from the GS to the ES with an escape time  $\tau_{ES}^{GS}$ , and from the ES to the RS with an escape time  $\tau_{RS}^{ES}$  through thermal excitations. The stimulated laser emission is operated on the GS only. It is noted that the model ignores the carrier transport process through the three-dimensional separate confinement heterostructure (barrier) as well as the direct carrier capture channel from the RS to the GS [35, 36]. Based on the schematic in Fig. 1, the rate equations describing the dynamics of the carrier numbers  $N_{RS,ES,GS}$ , the photon number  $S$ , and the phase of the electrical field  $\phi$  for the

Qdot laser are given by [37]:

$$\frac{dN_{RS}}{dt} = \frac{\eta I}{q} + \frac{N_{ES}}{\tau_{RS}^{ES}} - \frac{N_{RS}}{\tau_{ES}^{RS}} (1 - \rho_{ES}) - \frac{N_{RS}}{\tau_{RS}^{spont}} \quad (2)$$

$$\begin{aligned} \frac{dN_{ES}}{dt} = & \left( \frac{N_{RS}}{\tau_{ES}^{RS}} + \frac{N_{GS}}{\tau_{ES}^{GS}} \right) (1 - \rho_{ES}) - \frac{N_{ES}}{\tau_{RS}^{ES}} \\ & - \frac{N_{ES}}{\tau_{GS}^{ES}} (1 - \rho_{GS}) - \frac{N_{ES}}{\tau_{ES}^{spont}} \end{aligned} \quad (3)$$

$$\begin{aligned} \frac{dN_{GS}}{dt} = & \frac{N_{ES}}{\tau_{GS}^{ES}} (1 - \rho_{GS}) - \frac{N_{GS}}{\tau_{ES}^{GS}} (1 - \rho_{ES}) \\ & - \Gamma_p v_g g_{GS} S - \frac{N_{GS}}{\tau_{GS}^{spont}} \end{aligned} \quad (4)$$

$$\frac{dS}{dt} = \left( \Gamma_p v_g g_{GS} - \frac{1}{\tau_p} \right) S + \beta_{sp} \frac{N_{GS}}{\tau_{GS}^{spont}} + F_S(t) \quad (5)$$

$$\frac{d\phi}{dt} = \frac{1}{2} \Gamma_p v_g (g_{GS} \alpha_{GS} + g_{ES} k_{ES} + g_{RS} k_{RS}) + F_\phi(t) \quad (6)$$

where  $I$  is the pump current,  $\eta$  is the current injection efficiency,  $q$  is the elementary charge,  $\beta_{sp}$  is the spontaneous emission factor,  $\tau_{RS,ES,GS}^{spont}$  are the spontaneous emission times,  $\tau_p$  is the photon lifetime,  $\Gamma_p$  is the optical confinement factor, and  $v_g$  is the group velocity of light. The gain of each state is respectively expressed as [38]

$$\begin{aligned} g_{GS} &= \frac{a_{GS}}{1 + \xi \frac{S}{V_S}} \frac{N_B}{V_B} (2\rho_{GS} - 1) \\ g_{ES} &= a_{ES} \frac{N_B}{V_B} (2\rho_{ES} - 1) \\ g_{RS} &= a_{RS} \frac{D_{RS}}{V_{RS}} (2\rho_{RS} - 1) \end{aligned} \quad (7)$$

where  $a_{RS,ES,GS}$  are the differential gains,  $\xi$  is the gain compression factor,  $V_S$  is the volume of the laser field inside the cavity,  $N_B$  is the total number of dots,  $V_B$  is the volume of the active region,  $D_{RS}$  is the total number of states in the RS, and  $V_{RS}$  is the volume of the RS [39].  $\rho_{GS,ES,RS}$  are the carrier occupation probabilities in the GS, the ES, and the RS, which are given by  $\rho_{GS} = \frac{N_{GS}}{2N_B}$ ,  $\rho_{ES} = \frac{N_{ES}}{4N_B}$ , and  $\rho_{RS} = \frac{N_{RS}}{D_{RS}}$ , respectively. In Eq. (6),  $\alpha_{GS}$  is the contribution of the GS carriers to the LBF, and the coefficients  $k_{ES,RS}$  are defined as [37, 40]

$$k_{ES,RS} = \frac{E_{GS}}{E_{ES,RS}} \left[ \frac{\hbar}{(E_{ES,RS} - E_{GS}) T_2} + \frac{(E_{ES,RS} - E_{GS}) T_2}{\hbar} \right]^{-1} \quad (8)$$

where  $E_{GS,ES,RS}$  are the state energies and  $T_2$  is the polarization dephasing time. The spontaneous emission noise of the laser light is taken into account through the Langevin noise sources  $F_S(t)$  to the photon number in Eq. (5) and  $F_\phi(t)$  to the phase in Eq. (6), respectively [41]. The auto- and cross-correlations of the two noise sources are

$$\begin{aligned} \langle F_S(t) F_S(t') \rangle &= U_S \delta(t - t') \\ \langle F_\phi(t) F_\phi(t') \rangle &= U_\phi \delta(t - t') \\ \langle F_S(t) F_\phi(t') \rangle &= 0 \end{aligned} \quad (9)$$

with the correlation variances being

$$\begin{aligned} U_S &= 2S \frac{\beta_{sp} N_{GS}}{\tau_{GS}^{spont}} \\ U_\phi &= \frac{1}{2S} \frac{\beta_{sp} N_{GS}}{\tau_{GS}^{spont}} \end{aligned} \quad (10)$$

It has been well established that the random carrier generation and recombination noises have little contribution in comparison with the spontaneous emission noise in Qwell lasers [41–43]. This is because that the carrier fluctuation is mainly induced by the photon variation (due to spontaneous emission noise) through the stimulated emission process, which is much stronger than the carrier noise effect [44]. Therefore, we believe that the carrier noises also have negligible contribution in Qdot lasers, and thus are not considered in Eqs. (2)-(4). On the other hand, this will be studied in details in the future work. In addition to the above quantum noises, excessive flicker noises at low frequencies (usually less than 1.0 MHz) broaden the spectral linewidth as well [45], and its relation with the spectral lineshape can refer to [46]. However, the discussion of the flicker noises is beyond the scope of this article, which does not affect the conclusions.

### 3. Results and discussion

Using the above rate equation model, we study the frequency noise (FN) characteristics of an InAs/InP Qdot laser [38]. The material and optical parameters of the laser used in the simulations are listed in Table 1. Through a standard small-signal analysis of rate equations (2)-(6) with perturbation sources of the Langevin noises  $F_S(t)$  and  $F_\phi(t)$ , we obtain the phase variation of the laser field  $\delta\phi(t) = \delta\phi(\omega) e^{j\omega t}$ , with  $\delta\phi(\omega)$  being the phase variation in the frequency domain and  $\omega$  being the angular frequency [20]. The FN spectrum of the Qdot laser is then calculated by  $FN(\omega) = |\frac{j\omega}{2\pi} \delta\phi(\omega)|^2$ .

Figure 2(a) shows the double-sided FN spectra of the Qdot laser at pump currents  $1.2\times$ ,  $1.6\times$ , and  $2.8\times I_{th}$ , with the lasing threshold at  $I_{th} = 49$  mA. The FN exhibits a pronounced peak around the relaxation resonance frequency  $f_R$ . The peak amplitude reduces at a high pump current due to the increase of the damping factor [20]. At frequencies beyond the resonance peak, the FN decreases to a constant level, which is solely determined by the spontaneous emission. Therefore, the full width at half maximum (FWHM) of the Schawlow-Townes linewidth is expressed as  $\Delta\nu_{ST} = 2\pi FN|_{f \gg f_R}$  with  $\omega = 2\pi f$  [44]. On the other hand, the FN spectrum below the resonance frequency is determined by not only the spontaneous emission but also the carrier fluctuations through the phase-amplitude coupling effect, and thus the total optical linewidth is given by  $\Delta\nu_{OL} = 2\pi FN|_{f < f_R}$  [44]. Based on the above relations, Fig. 2(b) shows both  $\Delta\nu_{OL}$  (closed circles) and  $\Delta\nu_{ST}$  (open circles) as a function of the pump current. As expected, both linewidths decrease with the increased pump current owing to the enhanced output power. It is remarked that the flicker noises, the spectral hole burning and the carrier heating effects can lead to a linewidth floor or a re-broadening with increasing power in both Qwell and Qdot lasers [15, 47].

It is noted that the relation of the linewidths and the LBF in Eq. (1) is not only suitable for conventional bulk and Qwell lasers, but also for Qdot lasers. Therefore, the LBF of the Qdot laser can be obtained from both linewidths in Fig. 2(b). In this way, the closed circles in Fig. 3(a) present the extracted LBFs, which include the contribution of populations in the GS, the ES, and the RS. It shows that the LBFs slightly increase with the bias current from 0.76 at  $1.1\times I_{th}$  to 0.81 at  $3.6\times I_{th}$ . The triangles point out that the population in the RS has negligible contribution to the LBF, and hence to the phase noise of the Qdot laser. In contrast, the population in the ES dominates the contribution, and increases the LBF by more than 50% from that introduced by the resonant GS (squares). In comparison, the LBFs (open circles) calculated from the FM/AM

**Table 1. Material and Optical Parameters of the Qdot Laser**

Symbol	Description	Value
$E_{RS}$	RS transition energy	0.97 eV
$E_{ES}$	ES transition energy	0.87 eV
$E_{GS}$	GS transition energy	0.82 eV
$\tau_{RS}^{RS}$	RS to ES capture time	6.3 ps
$\tau_{ES}^{ES}$	ES to GS relaxation time	2.9 ps
$\tau_{ES}^{RS}$	ES to RS escape time	2.7 ns
$\tau_{GS}^{GS}$	GS to ES escape time	10.4 ps
$\tau_{RS}^{Spon}$	RS spontaneous emission time	0.5 ns
$\tau_{ES}^{Spon}$	ES spontaneous emission time	0.5 ns
$\tau_{GS}^{Spon}$	GS spontaneous emission time	1.2 ns
$\tau_p$	Photon lifetime	4.1 ps
$T_2$	Polarization dephasing time	0.1 ps
$\beta_{sp}$	Spontaneous emission factor	$1.0 \times 10^{-4}$
$a_{GS}$	GS Differential gain	$5.0 \times 10^{-15} \text{ cm}^2$
$a_{ES}$	ES Differential gain	$10 \times 10^{-15} \text{ cm}^2$
$a_{RS}$	RS Differential gain	$2.5 \times 10^{-15} \text{ cm}^2$
$\xi$	Gain compression factor	$2.0 \times 10^{-16} \text{ cm}^3$
$\Gamma_p$	Optical confinement factor	0.06
$\alpha_{GS}$	GS contribution to LBF	0.50
$N_B$	Total dot number	$1.0 \times 10^7$
$D_{RS}$	Total RS state number	$4.8 \times 10^6$
$V_B$	Active region volume	$5.0 \times 10^{-11} \text{ cm}^3$
$V_{RS}$	RS region volume	$1.0 \times 10^{-11} \text{ cm}^3$

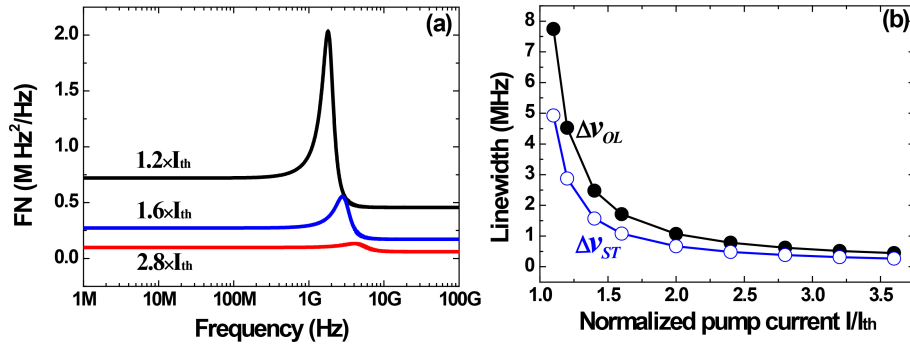


Fig. 2. (a) FN spectra at different pump currents; (b) Optical linewidth ( $\Delta\nu_{OL}$ ) and Schawlow-Townes linewidth ( $\Delta\nu_{ST}$ ) as a function of the pump current normalized to the threshold current.

method (see [37] in details) significantly increase from 0.79 to 1.1, which are larger than the LBFs obtained from the linewidth. This is in agreement with the observation in [31]. It means that a Qdot laser may simultaneously exhibit a narrow spectral linewidth (low LBF value from the linewidth) as discussed in the introduction, while produces a large frequency chirp (high LBF value from the FM/AM method) under direct current modulation [48]. In order to understand the above behaviours in Fig. 3(a), we can derive the analytical formula of the Qdot laser's LBF through the noise-induced phase ( $\delta\phi$ ) and gain ( $\delta g_{GS}$ ) variations using the small-signal

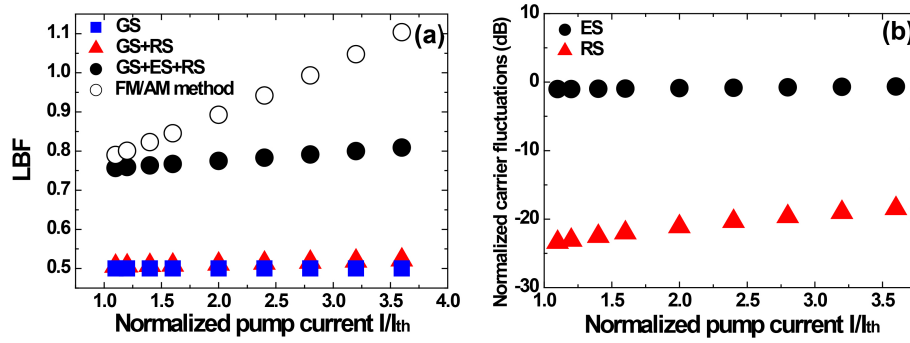


Fig. 3. (a) The LBF obtained from the optical linewidth: squares—the contribution of the GS; triangles—the contribution of the GS and the RS; closed circles—the contribution of the GS, the ES, and the RS. The open circles are the LBFs extracted from the FM/AM method. (b) Normalized carrier fluctuations in the ES (circles) and in the RS (triangles) with respect to that in the GS. The fluctuations are taken at a frequency of 1.0 MHz.

analysis [37]:

$$\alpha = \left| \frac{2}{\Gamma_p v_g} \frac{\omega \delta \phi(\omega)}{\delta g_{GS}(\omega)} \right| \approx \alpha_{GS} + \frac{k_{ES}}{2} \frac{a_{ES} \delta N_{ES}}{a_{GS}^P \delta N_{GS}} + 2k_{RS} \frac{a_{RS} \delta N_{RS} V_B}{a_{GS}^P \delta N_{GS} V_{RS}} \quad (11)$$

where  $a_{GS}^P = \frac{a_{GS}}{1 + \xi \frac{s}{V_S}}$  is the differential gain of the GS considering the gain compression effect,  $\delta N_{RS,ES,GS}$  are the carrier fluctuations due to the perturbation. This equation shows that the LBF of Qdot laser originates from three parts: the GS carrier contribution ( $\alpha_{GS}$ ), the ES carrier relative fluctuation ( $\frac{\delta N_{ES}}{\delta N_{GS}}$ ), and the RS carrier relative fluctuation ( $\frac{\delta N_{RS}}{\delta N_{GS}}$ ). The contributions of off-resonant carrier fluctuations to the LBF are weighted by the coefficients  $k_{ES,RS}$  and the differential gains. Figure 3(b) shows that the optical-noise induced carrier fluctuation in the ES (circles) is similar to that in the GS, which can be attributed to the strong coupling between the two states of small energy separation (50 meV). In contrast, the fluctuation in the RS (triangles) is more than 20 dB weaker resulting from the large energy separation (150 meV). This leads to the dominating contribution of the ES and the negligible contribution of the RS to the LBF in Fig. 3(a). It is apparent that the LBF can be reduced by enlarging the energy separation between the GS and the off-resonant states, which decreases both the carrier fluctuations and the coefficients  $k_{ES,RS}$ . It is remarked that the carrier fluctuations in InAs/GaAs Qdot lasers can be different due to the stronger confinement of electrons and the weaker confinement of holes [49].

The carrier capture rate from the RS to the ES, and the relaxation rate from the ES to the GS have been demonstrated to have significant influences on the dynamics of Qdot lasers, such as the modulation response, the frequency chirp, as well as the nonlinear laser dynamics [50–52]. Figure 4 shows the impact of the relaxation time on the linewidths [Fig. 4(a)] and on the LBF [Fig. 4(b)], where the capture time is kept as  $\tau_{ES}^{RS} = 2.17 \times \tau_{GS}^{ES}$ . It is found that both the two linewidths and the LBF have little change for relaxation times below 10 ps. Beyond 10 ps, the slow relaxation rate increases the linewidths and the LBF due to the accumulation of carriers in the off-resonant states as well as the reduction of photons. In practice, the carrier scattering times are usually less than 10 ps above the lasing threshold. Therefore, the phase noise of Qdot lasers has low sensitivity to the carrier scattering rates.

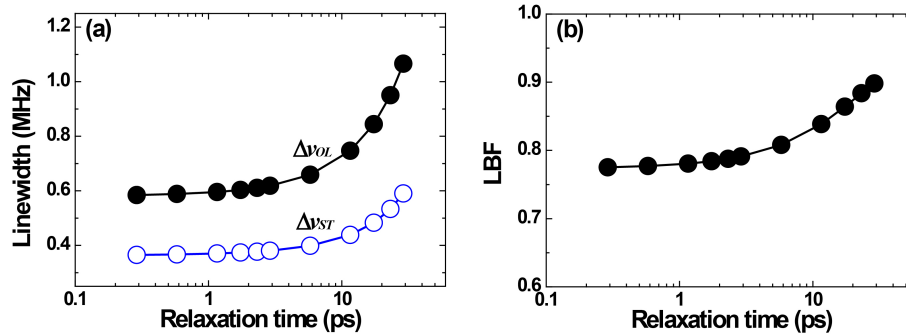


Fig. 4. (a) The optical linewidth and (b) the LBF as a function of the carrier relaxation time. The bias current is fixed at  $2.8 \times I_{th}$ .

#### 4. Conclusion

Based on the above discussions, Qdot lasers can exhibit a narrow spectral linewidth owing to the discrete density of states. In order to suppress the phase noise, one can not only employ techniques discussed in the introduction, but also reduce the LBF by proper quantum engineering of the Qdot states. A stronger (lateral) confinement of Qdots leads to a larger energy separation between the GS and the off-resonant states [53–55]. This reduces both the weighting coefficients  $k_{ES,RS}$  and the off-resonant carrier fluctuations in Eq. (11), and therefore the phase noise of the Qdot laser is suppressed. In addition, the role of off-resonant states can be demonstrated by measuring the phase noises of Qdot lasers with different Qdot confinement energies.

In conclusion, we demonstrate the contribution of off-resonant populations in the ES and the in RS to the phase noise of Qdot lasers through the phase-amplitude coupling effects. The ES dominates the contribution due to strong carrier fluctuations induced by the optical noise, while the influence of carriers in the RS is negligible owing to the large energy separation with the GS. Especially, the optical-noise induced LBF is smaller than the LBF induced by current modulation. In addition, it is found that the carrier scattering rates have little impact on the phase noise of Qdot lasers. These results are of great significance for the design of low-noise Qdot lasers for applications in coherent communication systems and in radio-over-fiber networks. Future work will study the carrier noise contribution to the phase noise, and measure the phase noise spectrum of Qdot lasers in experiment to confirm the theoretical observations. In addition, Qdot lasers operated on the ES emission will be investigated as well, which are expected to exhibit even lower phase noise based on our previous work [38].

#### Funding

The National Natural Science Foundation of China (NSFC) (61308002), the Research Grant Council of Hong Kong, China (CityU 11201014), the European Office of Aerospace Research and Development (FA9550-15-1-0104), and the Research Startup Fund of ShanghaiTech, China (F-0203-16-005).